Experimental bulk energy bands for diamond using $h\nu$-dependent photoemission

F. J. Himpsel, J. F. van der Veen, and D. E. Eastman

IBM Thomas J. Watson Research Center, Yorktown Heights, New York 10598

(Received 17 March 1980)

Using photon-energy-dependent photoemission techniques with a diamond (111)-(1 × 1) crystal surface, we have determined critical points of energy bands at Γ and L ($\Gamma_1 = -21$ eV, $L_1 = -12.8$ eV, $L_2' = -15.2$ eV, $\Gamma_{15} = +6.0$ eV, $\Gamma_2' = +15.3$ eV, $L_2' = +20$ eV, $\Gamma = +24$ eV with respect to the top of the valence band Γ_{25}'). Recent *ab initio* calculations agree with our results within 0.6 eV for the valence bands and show qualitative agreement for the empty conduction bands. The final bands are observed to be non-free-electron-like up to at least $+30$ eV.

I. INTRODUCTION

Diamond has been of considerable interest as a prototype for theoretical energy-band studies of semiconductors.[1-16] First-principles calculations are feasible because of the low number of electrons involved. Also, diamond has been a test case for various computational methods and potentials,[10,14] in particular for nonlocal pseudopotentials.[9,16] Recently, diamond has been used as a model semiconductor for a self-consistent Schottky-barrier calculation.[17] Several band calculations of intrinsic surface states and reconstruction and relaxation effects for the diamond (111) surface have been reported,[18-20] including recent self-consistent pseudopotential calculations.[16,17]

However, experimental data for the energy bands of diamond are rather sparse. Optical constants have been measured (see Ref. 21) which show an indirect band gap of 5.5 eV (Ref. 22) between the valence-band maximum at the Brillouin-zone center and the conductor-band minimum Δ_1^{min}, which has been located at $(0.8, 0, 0)2\pi/a$ from neutron diffraction studies.[23,24] The valence-band density of states has been studied via x-ray photoelectron spectroscopy (XPS) (Ref. 25, 26) and soft x-ray emission spectroscopy (SXS),[27] with XPS sampling mostly s-like states and SXS sampling p-like states. Previous data obtained via ultraviolet photoelectron spectroscopy (UPS) (Ref. 28) have suffered from having surfaces disordered by ion bombardment.

The diamond surface has been studied by low-energy electron diffraction (LEED) and energy loss spectroscopy (see Ref. 29). Diamond (111) surfaces with both unreconstructed (1×1) and reconstructed (2×2) structures have been observed (Refs. 29 and 30), the latter being prepared by a high temperature anneal of a natural (111) crystal face. Recently, we have found that diamond (111) prepared with an unreconstructed (1×1) surface

has a negative electron affinity[31]; i.e., the bottom of the conduction band lies above the vacuum level.

In this paper, we present angle-integrated and angle-resolved UPS data for a diamond (111)-(1×1) surface. UPS spectra depend strongly on the photon energy, which was varied in the range $10 \lesssim h\nu \lesssim 100$ eV using synchrotron radiation. These spectra have shown that direct interband transitions prevail in diamond. From the photon-energy dependence and angular dependence of spectral features in the spectra, we have obtained bulk energy-band critical points at Γ and L for both valence and final conduction-band states. Lifetimes of final states at energies between 15 and 25 eV above the top of the valence band have been determined to be $\sim(2-4)\times10^{-16}$ sec, i.e., comparable to lifetimes in metals at that energy.

Three recent *ab initio* calculations by Painter *et al.*,[11] Zunger *et al.*,[15] and by Ihm *et al.*,[16] have reported critical points at Γ and L which agree within 0.6 eV with our experimental valence-band critical points and agree qualitatively with our experimental final-state conduction-band critical points. The final-state energy bands within ~30 eV of the band gap are rather flat and deviate strongly from free-electron-like behavior.

II. EXPERIMENTAL METHODS

The natural (111) surface of a single crystal conductive diamond boron-doped, type-IIb, about $6\times5\times4$ mm^3 in size, was studied. The surface was prepared in a manner suggested by Lurie and Wilson,[29] i.e., the crystal was washed ultrasonically in acetone and then mounted in the photoelectron spectrometer. After an ~150℃ bakeout, a sharp unreconstructed (1×1) LEED pattern was observed (at all measured beam energies $75 \lesssim E \lesssim 300$ eV). After subsequent heating to ~900℃ in a vacuum of ~1×10^{-10} Torr, the overall LEED pattern did not change and adsorbate structures seen in the photo-

emission spectra below the valence band for the "as-mounted" diamond disappeared. Auger spectra showed only a trace of oxygen (<5% peak to peak of the carbon Auger signal). This does not preclude the formation of CH species or disordered carbon at the surface which likely were present to some degree since no intrinsic surface states were seen. However, when a disordered surface was obtained via heating by electron bombardment, LEED spectra for kinetic energies below 200 eV (where the escape depth is short) showed very low intensity LEED patterns with little contrast, and photoemission features characteristic of the diamond (111)-(1×1) structure disappeared. In particular, a spike in the photoemission secondary electron distribution at the bottom of the conduction band associated with the negative electron affinity of diamond (111)-(1×1) vanished.[30,31] Upon heating to temperatures above ~1000℃ a (2×2) [or (1×2)] reconstruction is observed which is accompanied by the appearance of diamond surface states near the top of the valence band.[30] Although cleaner than the 1×1 surface, this (2×2) surface is less suitable for determining bulk band-structure features because of extra surface-state emission and surface umklapp effects.

Photoemission measurements were made using synchrotron radiation from the 240 MeV storage ring of the University of Wisconsin—Madison and a display-type electron energy analyzer which analyzes all emitted electrons within a 1.8 steradian cone (86° full angle).[32] The photon-energy resolution varied from 0.2 (low $h\nu$) to 0.4 eV (high $h\nu$) and the electron energy resolution from 0.1 to 0.2 eV. Angle-resolved spectra were taken using the same analyzer with an angular acceptance of ≤8° full width.

The position of the top of the valence band ($\Gamma_{25'}$) was determined using the measured low-energy cutoff of the spectra (which represents the bottom of the conduction band) together with the known band gap. This simple relationship occurs because diamond (111)-(1×1) has a negative electron affinity, as we have shown previously.[31] A value of 5.5 eV was used for the band gap, which is the value determined from optical data[22] as well as from the photoyield threshold at 5.5 eV.[31] We find the Fermi level E_F to be ~1 eV above the top of the valence-band maximum E_v for the (1×1) surface and ~1.5 eV above E_v for the (2×2) surface.

III. EXPERIMENTAL RESULTS AND DISCUSSION

Figure 1 presents an overview set of angle-integrated photoemission energy distribution curves (EDC's) at various photon energies $h\nu$. For high photon energies ($h\nu > 50$ eV), EDC's show spectral
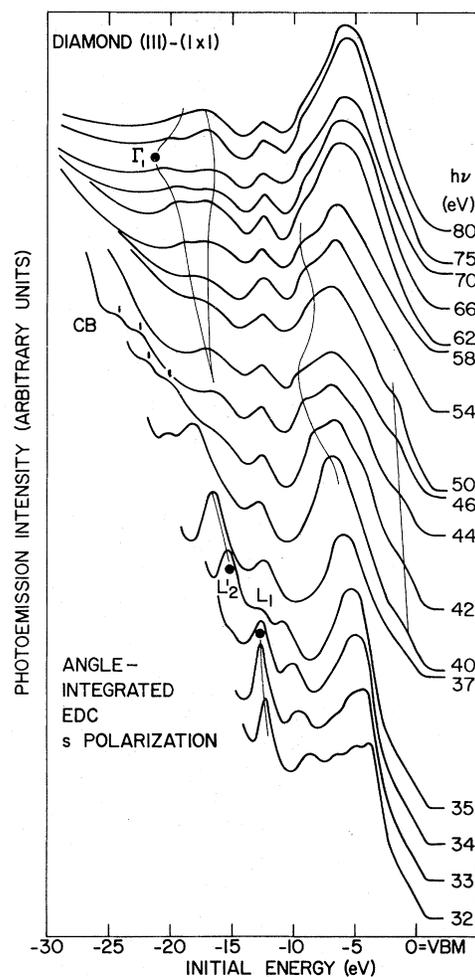

FIG. 1. Angle-integrated photoelectron spectra for diamond (111)-(1 × 1) for photon energies $h\nu$ in the range $32 \leq h\nu \leq 80$ eV (s-polarized light). Characteristic $h\nu$-dependent structures are marked which are used to obtain the points Γ_1, L_1, and L_2' of the valence band (dots). Energies are referenced to the valence-band maximum $\Gamma_{25}' \equiv E_v$. Features labeled CB are structures in the secondary electron spectra.

features extending over the uppermost 20 eV of the spectrum which correspond to the density-of-states features of the diamond valence bands (see, e.g., the calculated density of states in Refs. 11 and 16). For photon energies below 50 eV, spectral features change rapidly with $h\nu$. This is due to the effect of interband transitions into non-free-electron-like final bands. Using a theoretical analysis of the type performed for Ge,[33] these spectra can be interpreted and compared with band-structure calculations. Information concerning critical points can be extracted without detailed analysis: for $h\nu \simeq 70$ eV a structure is observed near −20 eV (measured relative to E_v) which disperses with $h\nu$.

There is a minimum in the dispersion (−21 eV at $h\nu \sim 71$ eV. This is assigned to the bottom of the valence band (Γ_1). Adding the photon energy $h\nu \sim 71$ eV to the initial energy, one obtains a final-state Γ point at +50 eV. A structure is observed at an initial energy $E_i = -12.8$ eV for $h\nu \leqslant 34$ eV. The rapid increase in intensity of this structure from $h\nu = 35$ to $h\nu = 34$ eV is associated with the onset of direct transitions from the valence band $\Gamma'_{25}L_1$ into the final band $\Gamma'_2L'_2$ near L (see Figs. 1 and 2). A second structure at $E_i = -15.2$ eV turns on for $h\nu \geqslant 35$ eV. This structure can be identified with transitions from the valence band $\Gamma_1L'_2$ into the same final band $\Gamma'_2L'_2$. The onset at $h\nu = 35$ eV is also associated with a transition at the L point. Thus, from the onset or disappearance of these two structures, we obtain the two initial-state L points (L'_2 at −15.2 eV, L_1 at −12.8 eV), and then obtain the final-state L point ($L'_2 = +20$ eV) by adding the corresponding photon energies to the observed initial-state energies.

A second method for obtaining information about the empty final bands is shown in Fig. 3. By varying the photon energy with the initial-state energy held fixed at the top of the valence band Γ'_{25}, in an angle-resolved constant-initial-state spectrum (ARCIS), two empty Γ points are reached via direct transitions Γ'_{25}. By comparing with recent *ab initio* calculations (Fig. 2), we assign the peak at $h\nu$

FIG. 3. Constant-initial-state spectrum (CIS) for photoelectrons emitted normal to the diamond (111)-(1 ×1) surface (p-polarized light). The initial energy is held fixed at the top of the valence band ($\Gamma'_{25} = E_v$). By varying the photon energy $h\nu$, transitions into various final bands at Γ are determined (e.g., $\Gamma'_{25} \rightarrow \Gamma'_2$ at $h\nu = 15.3$ eV).

$= 15.3$ eV in Fig. 3 to the transition $\Gamma'_{25} \rightarrow \Gamma'_2$. The peak at $h\nu = 24$ eV in Fig. 3 is due to a transition to a higher band at Γ. This spectral peak is broader than the lower energy peak and is asymmetric. This asymmetry could be due in part to a second unresolved band at Γ (e.g., as found in Ref. 16) or could be due to energy-dependent lifetime effects and matrix elements.

The finite lifetime τ of an electron in the conduction band (due to electron-electron scattering at energies $\gtrsim 2E_{\mathrm{gap}}$ above Γ'_{25}) broadens the transitions observed in Fig. 3 by an amount $\Delta E = \hbar/\tau$ (ΔE = full width at half maximum). Since the initial-state lifetime broadening is negligible at the top of the valence band, we directly obtain final-state lifetimes[34,35]: i.e., $\Delta E = 1.7$ eV or $\tau \sim 4 \times 10^{-16}$ sec for the $\Gamma'_2L'_2$ final-state band at ~15 eV above the top of the valence band and $\Delta E \simeq 3.5$ eV or $\tau \simeq 2 \times 10^{-16}$ sec for the final Γ state at 24 eV (neglecting the possibility of a second band). In a similar fashion, from ARCIS with initial states near L'_2, L_1, we have determined $\Delta E \simeq 2.5$ eV, or $\tau \simeq 1.3 \times 10^{-16}$ sec, for a final state 20 eV above E_v at the L point. In this case, the finite initial-state lifetime ($\hbar/\tau \sim 1.3$ eV for L'_2, L_1) affects the measurement of the final-state lifetime to some degree. These final-state lifetimes are in the same range as observed for metals.[34,35]

A third source of information about conduction-band features is given by the energy distribution of secondary electrons. Spectral features (e.g., maxima) in the spectrum of secondaries can be observed at local conduction-band minima either because of scattering effects or because of high densities of states associated with flat conduction
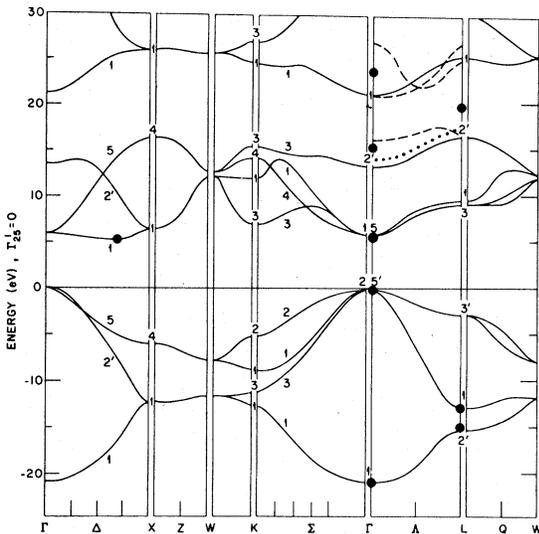

FIG. 2. Calculated energy bands for diamond by Painter *et al.* (Ref. 11) are compared with experimental critical points (dots). Several conduction bands along ΓL calculated by Ihm *et al.* (Ref. 16) are shown as dashed lines. The dotted line is from the calculation by Zunger *et al.* (Ref. 15). For the valence bands, the three calculations are very similar.
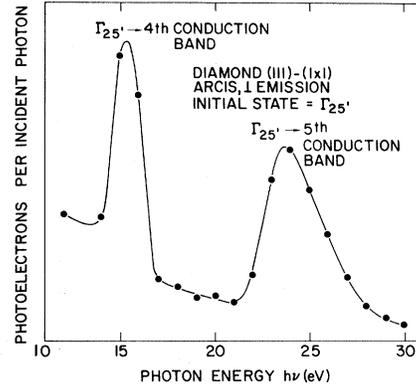
TABLE I. Experimental critical points for diamond energy bands (in eV relative to the top of the valence band $\Gamma'_{25} \equiv E_v$).

Γ_1	-21 ± 1	(direct transition, see Fig. 1)
Γ_{15}	$+6.0 \pm 0.2$	(secondary electron structure)
Γ'_2	$+15.3 \pm 0.5$	(direct transition, see Fig. 3)
Γ	$+24 \pm 1.5$ [a]	(direct transition, see Fig. 3)
Γ	$+50 \pm 4$	(direct transition, see Fig. 1)
L'_2	-15.2 ± 0.3	(direct transition, see Fig. 1)
L_1	-12.8 ± 0.3	(direct transition, see Fig. 1)
L'_2	$+20 \pm 1.5$	(direct transition and secondary electron structure, see Fig. 1)
Δ_1^{min}	$+5.5 \pm 0.05$	(photoelectric yield threshold, see Ref. 31)

[a] Possibly two unresolved Γ points of unknown symmetry.

bands.[36] Spectral features are observed at 20 and 22 eV above E_v in normal emission spectra (e.g., see the ticmarks labeled CB in Fig. 1) which are consistent with high densities of states near L'_2 and the bottom of the 5th conduction band, respectively. When direct transitions into those final states are possible, we find them strongly enhanced (e.g., around $h\nu = 35$ eV in Fig. 1; compare the discussion above). Two structures in the secondary distribution (at 12 and 13.5 eV, not shown in Fig. 1) are seen for off normal emission. Since $\vec{k}_\parallel$ is conserved for a specular surface, these features are attributed to points in $\vec{k}$ space not along the ΓL line (ΓL corresponds to $\vec{k}_\parallel = 0$, i.e., normal emission). A 0.5-eV-wide spike has been observed at the bottom of the secondary electron spectrum (see Ref. 30). This could be due to the high density of states in the flat $\Gamma_{15}\Delta_1 X_1$ band along which the conduction-band minimum occurs. This tentative assignment would place the top of this band (X_1 or Γ_{15}) about 0.5 eV above the conduction-band minimum, i.e., 6.0 eV above the top of the valence band. This assignment is very uncertain, however, due to predominant phonon scattering effects which strongly affect the line shape at the bottom of the conduction band.

In Table I we summarize our findings for critical points of diamond along ΓL. Upon comparing three recent ab initio calculations[11,15,16] with our experimental critical points, we find very good agreement for the valence bands (better than 0.6 eV for all measured points). Calculated empty band critical points are less accurate but are qualitatively similar to our experimental results.

Calculation and experiment both show that the final bands up to ~30 eV (i.e., 1.5 times the valence bandwidth) above the valence-band maximum are rather flat and non-free-electron-like. Even the experimental Γ point at +50 eV is far from any free-electron-like Γ point. For other semiconductors (e.g., GaAs) a similar conduction-band behavior has been found for the corresponding energy range (scaled by the valence-bandwidth). The flat final bands can be interpreted as the antibonding $2s2p$-like orbitals formed from the two C atoms in the unit cell.[37] For diamond, the antibonding $2s$ orbitals (associated with Γ'_2) lie well above the antibonding $2p$ orbitals (associated with Γ_{15}). Diamond shares this ordering with Si according to present calculations, whereas Ge and III-V compounds (e.g., GaAs) have the reverse ordering.

For diamond, the energy bands calculated for the ground state agree quite well with the photoemission data, which probe excited states. This is in striking contrast with wide-gap heteropolar materials (e.g., LiF; see Refs. 38 and 39). One method for determining excited-state effects (in particular excitonic effects) is to compare results obtained from interband transitions (with a hole present in the valence band) to results obtained from the spectrum of secondary electrons (no hole present). For the L'_2 conduction-band point we are able to make such a comparison and find no difference within the experimental accuracy, which is rather limited (± 1.5 eV for this point).

[1]L. Kleinman and J. C. Phillips, Phys. Rev. <u>125</u>, 819 (1962).

[2]F. Bassani and M. Yashimine, Phys. Rev. <u>130</u>, 20 (1963).

[3]W. Saslow, T. K. Bergstresser, and M. L. Cohen, Phys. Rev. Lett. <u>16</u>, 354 (1966).

[4]R. Keown, Phys. Rev. <u>150</u>, 586 (1966).

[5]F. Herman, R. L. Kartum, and C. D. Kuglin, Int. J. Quantum Chem. <u>15</u>, 533 (1967).

[6]L. Saravia and D. Brust, Phys. Rev. <u>170</u>, 683 (1968).

[7]W. von Haeringen and H. G. Junginger, Solid State Commun. <u>7</u>, 1135 (1969).

[8]R. N. Euwema and D. J. Stukel, Phys. Rev. B <u>1</u>, 4692 (1970).

[9]L. A. Hemstreet, C. Y. Fong, and M. L. Cohen, Phys. Rev. B <u>2</u>, 2054 (1970).

[10]R. C. Chaney, C. C. Lin, and E. E. Lafon, Phys. Rev. B <u>3</u>, 459 (1971).

[11]G. S. Painter, D. E. Ellis, and A. R. Lubinsky, Phys. Rev. B <u>4</u>, 3610 (1971).

[12]J. R. P. Neto and L. G. Ferreira, J. Phys. C <u>6</u>, 3420 (1973).

[13]P. W. Kervin and E. E. Lafon, J. Chem. Phys. <u>58</u>, 1535 (1973).

[14]J. R. Leite, B. I. Bennett, and F. Herman, Phys. Rev. B <u>12</u>, 1466 (1975).

[15]Alex Zunger and A. J. Freeman, Phys. Rev. B <u>15</u>, 5049 (1977).

[16]J. Ihm, S. G. Louie, and M. L. Cohen, Phys. Rev. B <u>17</u>, 769 (1978).

[17]J. Ihm, S. G. Louie, and M. L. Cohen, Phys. Rev. Lett. <u>40</u>, 1208 (1978).

[18]D. Pugh, Phys. Rev. Lett. <u>12</u>, 390 (1964).

[19]L. C. Snyder and Z. Wassermann, Surf. Sci. <u>71</u>, 407 (1978).

[20]W. S. Verwoerd and F. J. Kok, Surf. Sci. <u>80</u>, 89 (1979).

[21]R. A. Roberts and W. C. Walker, Phys. Rev. <u>161</u>, 730 (1967)

[22]C. D. Clark, P. J. Dean, and P. V. Harris, Proc. R. Soc. London A<u>277</u>, 312 (1964).

[23]P. J. Dean, E. C. Lightowlers, and D. R. Wight, Phys. Rev. <u>140</u>, A352 (1965).

[24]E. O. Kane, Phys. Rev. <u>146</u>, 558 (1966).

[25]R. G. Cavell, S. P. Kowalczyk, L. Ley, R. A. Pollak, B. Mills, D. A. Shirley, and W. Perry, Phys. Rev. B <u>7</u>, 5313 (1973).

[26]F. R. McFeely, S. P. Kowalczyk, L. Ley, R. G. Cavell, R. A. Pollack, and D. A. Shirley, Phys. Rev. B <u>9</u>, 5268 (1974).

[27]G. Wiech and E. Zöpf, in *Electronic Density of States*, Natl. Bur. Stand. Spec. Publ. 323 (U.S. GPO, Washington, D. C., 1969), p. 335; M. Umeno and G. Wiech, Phys. Status Solidi B <u>59</u>, 145 (1972).

[28]S. Evans and J. M. Thomas, Proc. R. Soc. London A<u>353</u>, 103 (1977).

[29]P. G. Lurie and J. M. Wilson, Surf. Sci. <u>65</u>, 453 (1977).

[30]F. J. Himpsel, D. E. Eastman, and J. F. van der Veen, J. Vac. Sci. Technol. (to be published).

[31]F. J. Himpsel, J. A. Knapp, J. A. Van Vechten, and D. E. Eastman, Phys. Rev. B <u>20</u>, 624 (1979).

[32]D. E. Eastman, J. J. Donelon, N. C. Hien, and F. J. Himpsel, Nucl. Instrum. Methods (to be published).

[33]W. D. Grobman, D. E. Eastman, and J. L. Freeouf, Phys. Rev. B <u>12</u>, 4405 (1975).

[34]D. E. Eastman, J. A. Knapp, and F. J. Himpsel, Phys. Rev. Lett. <u>41</u>, 825 (1978).

[35]F. J. Himpsel and W. Eberhardt, Solid State Commun. <u>31</u>, 747 (1979).

[36]F. J. Himpsel and W. Steinmann, Phys. Rev. B <u>17</u>, 2537 (1978).

[37]J. C. Slater, *Quantum Theory of Molecules and Solids* (McGraw-Hill, New York, 1963).

[38]A. B. Kunz, in *Vacuum Ultraviolet Radiation Physics*, edited by E. E. Koch, R. Haensel, and C. Kunz (Pergamon, New York, 1974), p. 331.

[39]Alex Zunger and A. J. Freeman, Phys. Rev. B <u>16</u>, 2901 (1977).